

A Linear Branch Flow Model for Radial Distribution Networks and its Application to Reactive Power Optimization and Network Reconfiguration

Tianshu Yang, *Student Member, IEEE*, Ye Guo, *Senior Member, IEEE*, Lirong Deng, *Student Member, IEEE*, Hongbin Sun, *Fellow, IEEE*, and Wenchuan Wu, *Senior Member, IEEE*

Abstract—This paper presents a cold-start linear branch flow model named modified DistFlow. In modified DistFlow, the active and reactive power are replaced by their ratios to voltage magnitude as state variables, so that errors introduced by conventional branch flow linearization approaches due to their complete ignoring of the quadratic term are reduced. Based on the path-branch incidence matrix, branch power flows and nodal voltage magnitudes can be obtained in a non-iterative and explicit manner. Subsequently, the proposed modified DistFlow model is applied to the problem of reactive power optimization and network reconfiguration, transforming it into a mixed-integer quadratic programming (MIQP). Simulations show that the proposed modified DistFlow has a better accuracy than existing cold-start linear branch flow models for distribution networks, and the resulting MIQP model for reactive power optimization and network reconfiguration is much more computationally efficient than existing benchmarks.

Index Terms—Distribution network, power flow analysis, reactive power optimization, network reconfiguration, cold-start model

NOMENCLATURE

Sets

Φ_B	Set of all buses
Φ_C	Set of VAR compensators
Φ_L	Set of all branches
N_i	Set of neighboring buses of bus i
Ψ_i	Set of branches on the path of bus i
Ω_{ij}	Set of the buses with branch ij in its path to root bus
B_l	Set of the branches in the fundamental loop l
Θ_i	Set of the branches in the i th overlapping loop set

Indices and Parameters

l_{ij}	Branch between buses i and j
R_{ij}, X_{ij}	Resistance and reactance of branch ij
$\tilde{P}_i^G, \tilde{Q}_i^G$	Forecasted active and reactive power provided by DG at bus i

P_i^D, Q_i^D	Active and reactive power demand at bus i
$\bar{Q}_i^C, \underline{Q}_i^C$	Maximum and minimum reactive power provided by SVC at bus i
N_{node}	Number of buses ($N_{node} = \Phi_B $)
N_{root}	Number of root buses
N_i	Number of branches in i th overlapping loop set
L_i	Number of links in i th overlapping loop set
$\bar{V}_i, \underline{V}_i$	Upper and lower bound of voltage magnitude at bus i
$\bar{P}_{ij}, \bar{Q}_{ij}$	Upper bound of active and reactive power flow on branch ij
\bar{I}_{ij}	Upper bound of current of branch ij
$\bar{\delta}_{ij}$	Upper bound of voltage angle difference of branch ij
M	A large positive number

Variables

x_{ij}	Binary variable for branch status
V_i	Voltage magnitude at bus i
W_i	Auxiliary variable (approximate $1/V_i$)
δ_{ij}	Voltage angle difference between buses i and j
P_{ij}, Q_{ij}	Sending-end active and reactive power flow of branch ij
P_i, Q_i	Total active and reactive power injection at bus i
$\hat{P}_{ij}, \hat{Q}_{ij}$	Modified active and reactive power flow on branch ij
\hat{P}_i, \hat{Q}_i	Modified active and reactive power injection at bus i
\hat{P}_i^G, \hat{Q}_i^G	Modified active and reactive power injection provided by DG
\hat{Q}_i^C	Modified reactive power injection provided SVC

Vectors and Matrices

V_S	Voltage magnitude vector of branch sending ends
V_R	Voltage magnitude vector of branch receiving ends
W_R	Vector of auxiliary variable W_i
V_0	Column vector with all values equal to the voltage magnitude of PSP (the reference bus)
$\hat{P}_{Br}, \hat{Q}_{Br}$	Column vector of modified active and reactive power flow on branches
T	Path-branch incidence matrix for a radial network
P_N, Q_N	Diagonal matrix of active and reactive injected power
R_N, X_N	Diagonal matrix of branch resistance and reactance ($R_N = \text{diag}(R_{ij}), X_N = \text{diag}(X_{ij})$)

Corresponding author: H. Sun and Y. Guo.

T. Yang, Y. Guo, L. Deng, H. Sun and W. Wu are with the Smart grid and Renewable Energy Laboratory, Department of Tsinghua-Berkeley Shenzhen Institute (TBSI), Tsinghua University, Shenzhen 518055, Guangdong, China. (email: guo-ye@sz.tsinghua.edu.cn; shb@tsinghua.edu.cn).

H. Sun and W. Wu are also with the State Key Laboratory of Power Systems, Department of Electrical Engineering, Tsinghua University, Beijing 100084, China.

I. INTRODUCTION

WITH the fast expansion of network scale and the deep penetration of renewable energy sources, increasingly complex and uncertain distribution systems need better control and optimization, such as network reconfiguration [1], reactive power (VAR) optimization [2], and economic dispatch [3]. To that end, the power flow model is an essential analytical tool. However, the standard alternating current power flow (ACPF) model is nonlinear and may make the aforementioned optimization problems non-convex. Therefore, a linear power flow model with satisfactory accuracy and efficiency for distribution system analysis and optimization is of crucial importance.

One of the most widely used linear power flow (LPF) model is the direct current power flow (DCPF). Although the DCPF model has a good accuracy for transmission network analysis, it is not directly applicable to distribution networks [4]. Besides, this model is not suitable for applications where reactive branch flows, voltage magnitudes, or network losses are of primary concern, such as VAR optimization, automatic voltage control (AVC) [5], and network reconfiguration. Considering the characteristics of distribution systems, many LPF models have been developed.

On applicability, there are warm-start models (WSM) [6-9] and cold-start models (CSM) [3, 9-12]. The former kind of methods linearizes the ACPF model around the operating points, thus requiring pre-determined initial points. Cold-start models, on the contrary, do not assume initial operation points. Given certain AC initial points, power flow results of the warm-start models are generally more accurate than those of the cold-start models. However, in situations such as network reconfiguration where no reliable initial points are available, a cold-start model is necessary.

On the selection of state variables, there are bus injection models and branch flow models. The former is a standard model for power flow analysis and optimization. It focuses primarily on nodal variables rather than power flows on branches [13, 14]. Most existing LPF models fall into this category, such as [3, 8-12]. For linear branch-flow models, a widely-used one is the Simplified DistFlow (SD) model [15]. As a cold-start model, its accuracy is worse than those in [3, 8-12]. A warm-start three-phase LBF model with modeling of on-load-tap-changer of transformers is developed in [6]. This model can produce an accurate power flow result if an operating point is given. Another warm-start LBF model is proposed in [7] for solving the coordinated charging issues for electric vehicles.

There are also studies based on the ACPF model with convex relaxation techniques employed to ensure tractability. Paper [13, 14] set forth a second-order cone program (SOCP) method that uses the reactive power capability of solar plant inverters to regulate the voltage and minimize the network loss. Paper [1] formulated the VAR optimization and network reconfiguration problem as a mixed-integer SOCP. However, considering the high DG penetration and the control of VAR compensators, SOCP cannot guarantee a feasible solution if the power injections are within a limited range, nor the objectives violate the relaxation condition [1, 16, 17]. Thus this method is difficult to be generalized.

As for VAR optimization and network reconfiguration, it is not trivial to set a good initial point in all cases. Thus cold-start models become more attractive. However, current cold-start LBF models, such as simplified DistFlow, may not guarantee the optimal solution due to significant errors. There is still a gap towards an ideal approach for optimizing the operations in active distribution networks.

To bridge this gap, this paper proposes a cold-start linear branch flow model, referred to as modified DistFlow, for distribution systems. Based on the modified DistFlow, a mixed-integer quadratic programming (MIQP) is proposed for VAR optimization and network reconfiguration. The major contributions of the paper are two-fold:

(i) To address the challenge of dealing with the quadratic terms in the branch flow model, i.e., network losses, we take the ratios of the active and reactive power to voltage magnitude as state variables. Furthermore, the linearization on voltage differences is based on Taylor expansion, which has a satisfactory accuracy in a wide range of system states with relatively small errors. The modified DistFlow neither relies on the initial points nor requires any assumption related to the R/X ratio or voltage magnitudes. Besides, by introducing the path-branch incidence matrix, the modified DistFlow can be solved in an explicit close form for general radial distribution networks. To our best knowledge, the modified DistFlow is more accurate than all the existing cold-start LBF models in the literature.

(ii) With the modified DistFlow, the VAR optimization and network reconfiguration problem can be formulated as a MIQP problem. Compared with the MISOCP model in [1], our method can be applied to a wider range of issues and is much more efficient to solve.

The remainder of this paper is organized as follows. Section II derives the cold-start LBF model, first for a simple two-bus system, then for general distribution networks. Section III describes the MIQP model for VAR optimization and network reconfiguration. In Section IV, the proposed LBF model and the MIQP model for VAR optimization and network reconfiguration are compared with existing benchmarks on multiple standard and modified test systems.

II. LINEAR BRANCH FLOW MODEL

A. A Two-bus system

1) Branch flow equations of a two-bus system.

In this section, the relationship between the sending-end power flow P_{ij}, Q_{ij} and the receiving-end power flow P_{ji}, Q_{ji} of two connected buses are analyzed to derive and simplify the branch flow equations. Consider a single distribution line in Fig.1.

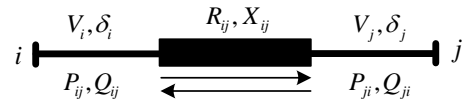


Fig. 1. A two-bus system.

Given the sending-end power flow and receiving-end power flow, the voltage drop along the distribution line can be calculated with either bus i or bus j as the phase angle reference.

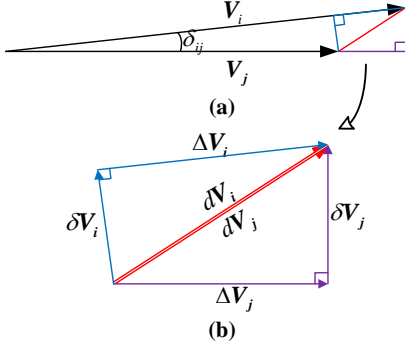


Fig. 2. Phasor diagram of the voltage drop. (Note that the figure based on the conditions $V_i > V_j$ and $\delta_{ij} > 0$ is to illustrate the following derivations (1)-(16), while the derivations are not limited to these conditions.)

As shown in Fig. 2, for the former case, components along the horizontal and vertical directions can be calculated as:

$$\Delta V_i = \frac{R_{ij}P_{ij} + X_{ij}Q_{ij}}{V_i}, \quad (1)$$

$$\delta V_i = \frac{X_{ij}P_{ij} - R_{ij}Q_{ij}}{V_i}. \quad (2)$$

For the latter case:

$$\Delta V_j = -\frac{R_{ij}P_{ji} + X_{ij}Q_{ji}}{V_j}, \quad (3)$$

$$\delta V_j = -\frac{X_{ij}P_{ji} - R_{ij}Q_{ji}}{V_j}, \quad (4)$$

where dV_i and dV_j are the voltage drop calculated by the sending-end power flow and receiving-end power flow, respectively. ΔV_i and δV_i are the rectangular components of dV_i ; Similarly, ΔV_j and δV_j are the rectangular components of dV_j .

In this paper, in order to obtain a linear branch flow model, the following assumption is made:

Assumption 1. The phase angle difference between two neighboring buses i and j is assumed to be zero. i.e., $\delta_{ij} \approx 0$.

Such an assumption is widely adopted in the literature, and verified by the simulations therein, e.g. [3, 9, 18]. Accordingly, there is:

$$\sin \delta_{ij} \approx \delta_{ij}. \quad (5)$$

The Taylor expansion of the cosine function around $\delta_{ij} = 0$ is:

$$\cos \delta_{ij} = 1 - \frac{1}{2}\delta_{ij}^2 + o(\delta_{ij}^2). \quad (6)$$

According to Fig. 2 (a), We have:

$$\Delta V_i = V_i - V_j \cos \delta_{ij} = V_i - V_j \left(1 - \frac{1}{2}\delta_{ij}^2 + o(\delta_{ij}^2) \right), \quad (7)$$

$$\Delta V_j = V_i \cos \delta_{ij} - V_j = V_i \left(1 - \frac{1}{2}\delta_{ij}^2 + o(\delta_{ij}^2) \right) - V_j. \quad (8)$$

By subtracting (8) from (7), we have:

$$\Delta V_i - \Delta V_j = \frac{1}{2}(V_i + V_j) \cdot \delta_{ij}^2 + o(\delta_{ij}^2). \quad (9)$$

Under Assumption 1, we make an approximation:

$$\Delta V_i \approx \Delta V_j. \quad (10)$$

Similarly, according to Fig. 2 (a), δV_i and δV_j satisfy:

$$\delta V_i = V_j \delta_{ij}, \quad (11)$$

$$\delta V_j = V_i \delta_{ij}. \quad (12)$$

By substituting (1)-(4) to (10)-(12), we obtain the relation between the power flow of the sending end and that of the receiving end:

$$\frac{P_{ij}}{V_i} = -\frac{P_{ji}}{V_j} - \frac{X_{ij}}{R_{ij}^2 + X_{ij}^2}(V_i - V_j)\delta_{ij}, \quad (13)$$

$$\frac{Q_{ij}}{V_i} = -\frac{Q_{ji}}{V_j} + \frac{R_{ij}}{R_{ij}^2 + X_{ij}^2}(V_i - V_j)\delta_{ij}. \quad (14)$$

These two equations can be simplified further. With Assumption 1, the terms containing δ_{ij} can be neglected:

$$\frac{P_{ij}}{V_i} \approx -\frac{P_{ji}}{V_j}, \quad (15)$$

$$\frac{Q_{ij}}{V_i} \approx -\frac{Q_{ji}}{V_j}. \quad (16)$$

Equations (15) and (16) show that the ratio between power flow and voltage magnitude of the sending end is approximately equal to that of the receiving end.

Remark:

Equations (15) and (16) form basic power flow equations of modified DistFlow. Although we assume that $\delta_{ij} \approx 0$ in Assumption 1, weaker assumptions are actually used in the derivation of (15) and (16). In Equation (10), the quadratic term of δ_{ij} is ignored. In Equations (15) and (16), the second term on the right-hand side of (13) and (14) are ignored, which are the product of $(V_i - V_j)$ and δ_{ij} . Note that the former term is also small. Therefore, our model enjoys better accuracy than many other models with the same assumption.

2) Voltage Equations of the two-bus system.

To visualize the non-linear nature of ACPF equations, we fix the voltage magnitude of bus i in the two-bus system as 1.0 p.u. and plot the change of V_j with P_j and Q_j as in Fig. 3 (a). From Fig. 3(a) we can see there is a strong non-linearity between V_j and P_j, Q_j . In contrast, if we replace P_j and Q_j with P_j/V_j and Q_j/V_j , the corresponding figure in Fig. 3(b) shows a much better linearity. Such observations inspire our idea of replacing P_j and Q_j with P_j/V_j and Q_j/V_j for the linearization on voltage equations.

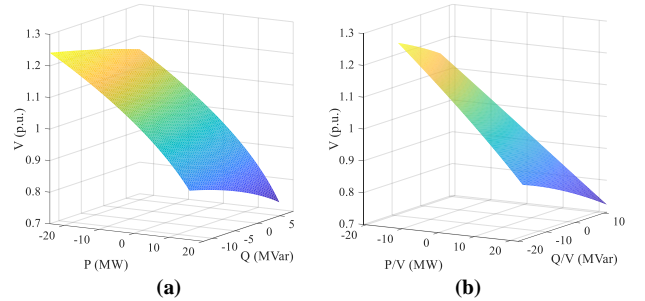


Fig. 3. Visualization of ACPF in the two-bus system.

The branch flow on the sending end is given by

$$P_{ij} = \frac{R_{ij}(V_i^2 - V_i V_j \cos \delta_{ij}) + X_{ij} V_i V_j \sin \delta_{ij}}{R_{ij}^2 + X_{ij}^2}, \quad (17)$$

$$Q_{ij} = \frac{X_{ij}(V_i^2 - V_i V_j \cos \delta_{ij}) - R_{ij} V_i V_j \sin \delta_{ij}}{R_{ij}^2 + X_{ij}^2}. \quad (18)$$

By combining (17) and (18), we have:

$$V_i - V_j \cos \delta_{ij} = R_{ij} \frac{P_{ij}}{V_i} + X_{ij} \frac{Q_{ij}}{V_i}, \quad (19)$$

$$V_j \sin \delta_{ij} = X_{ij} \frac{P_{ij}}{V_i} - R_{ij} \frac{Q_{ij}}{V_i}. \quad (20)$$

Under Assumption 1, (19) can be further simplified as:

$$V_i - V_j \approx R_{ij} \frac{P_{ij}}{V_i} + X_{ij} \frac{Q_{ij}}{V_i}. \quad (21)$$

Let

$$\hat{P}_{ij} = \frac{P_{ij}}{V_i}, \quad \hat{Q}_{ij} = \frac{Q_{ij}}{V_i}. \quad (22)$$

$$\hat{P}_i = \frac{P_i}{V_i}, \quad \hat{Q}_i = \frac{Q_i}{V_i}. \quad (23)$$

Then (21) becomes:

$$V_i - V_j = R_{ij} \hat{P}_{ij} + X_{ij} \hat{Q}_{ij}. \quad (24)$$

Equation (24) describes how voltage magnitude drops linearly along distribution lines. However, according to (23), \hat{P} and \hat{Q} are affine mappings of $1/V_i$ as the P and Q are fixed. Thus, variables V_i in (24) should be transformed to $1/V_i$.

Consider the function $f(\Delta V) = 1/(1 - \Delta V)$. Its Taylor series around zero is:

$$\frac{1}{1 - \Delta V} = \sum_{n=0}^{+\infty} (\Delta V)^n, \quad \|\Delta V\| < 1. \quad (25)$$

By neglecting high order terms and defining $V = 1 - \Delta V$, a linear approximation of $1/V$ is obtained:

$$\frac{1}{V} \approx 1 + \Delta V = 2 - V. \quad (26)$$

By substituting (26) to (24), we have:

$$\frac{1}{V_j} - \frac{1}{V_i} = R_{ij} \hat{P}_{ij} + X_{ij} \hat{Q}_{ij}. \quad (27)$$

Equation (27) is the voltage equation of the proposed modified DistFlow.

According to Taylor expansion, the error for the linearization on the left-hand side of (27) is:

$$\theta(V_i, V_j) = 100 \cdot \left\| \left(\frac{1}{V_i} - (2 - V_i) \right) - \left(\frac{1}{V_j} - (2 - V_j) \right) \right\|. \quad (28)$$

Generally, the voltage drop between two buses is small, and thus the error introduced by (26) will be small. For example, the error for $V_i = 0.8$ and $V_j = 0.82$ is around 1%.

B. Generalization

Next, we consider general distribution networks. A simple example of a distribution feeder where each bus only has one child-node is illustrated in Fig. 4:

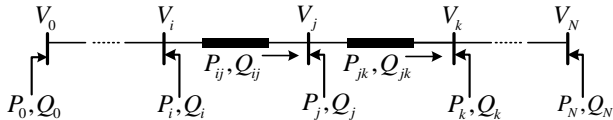


Fig. 4. One-line diagram of a main distribution feeder.

According to KCL, the sum of the injected power of a node is zero. Take bus j as an example. There are:

$$-\frac{P_{ji}}{V_j} = \frac{P_{jk}}{V_j} - \frac{P_j}{V_j}, \quad (29)$$

$$-\frac{Q_{ji}}{V_j} = \frac{Q_{jk}}{V_j} - \frac{Q_j}{V_j}. \quad (30)$$

By substituting (15) and (16) into (29) and (30), we have

$$\frac{P_{jk}}{V_j} = \frac{P_{ij}}{V_i} + \frac{P_j}{V_j}, \quad (31)$$

$$\frac{Q_{jk}}{V_j} = \frac{Q_{ij}}{V_i} + \frac{Q_j}{V_j}, \quad (32)$$

where (31) and (32) are the branch flow equations of the modified DistFlow.

Let W_i approximate $1/V_i$, and rewrite (23), (31) and (32). The modified DistFlow becomes:

$$\hat{P}_{jk} = \hat{P}_{ij} + \hat{P}_j, \quad (33)$$

$$\hat{Q}_{jk} = \hat{Q}_{ij} + \hat{Q}_j, \quad (34)$$

$$W_j - W_i = R_{ij} \hat{P}_{ij} + X_{ij} \hat{Q}_{ij}, \quad (35)$$

$$\hat{P}_i = P_i W_i, \quad (36)$$

$$\hat{Q}_i = Q_i W_i. \quad (37)$$

Equations (33)-(37) are the *modified DistFlow* equations, with the boundary conditions $\hat{P}_{N,N+1} = \hat{Q}_{N,N+1} = 0$ and $W_0(V_0)$.

After the model is solved, the branch flow P_{ij} and Q_{ij} can be calculated by:

$$P_{ij} = \frac{\hat{P}_{ij}}{W_i}, \quad Q_{ij} = \frac{\hat{Q}_{ij}}{W_i}. \quad (38)$$

Since the network is radial, the solution for the modified DistFlow equations can be obtained easily; for a radial network of the type shown in Fig. 4, the solutions of branch equations (33)-(34) are the following form:

$$\hat{P}_{ij} = - \sum_{k \in \Omega_{ij}} \hat{P}_k, \quad (39)$$

$$\hat{Q}_{ij} = - \sum_{k \in \Omega_{ij}} \hat{Q}_k. \quad (40)$$

Equations (33)-(34) and (39)-(40) are equivalent in many places. However, consider an optimization problem, if the network topology changes, only (33) and (34) can be employed.

To apply the proposed modified DistFlow to more general cases, the path-branch incidence matrix [19, 20] is employed. Accordingly, the modified DistFlow equations for general radial distribution networks can be written in an explicit matrix form.

A path-branch incidence matrix describes the incidence relations between all directed paths ending at the root node and the branches, where column i represents the path from bus i to the root bus. Namely, its entry (l_{ij}, k) is defined as:

$$T_{l_{ij}, k} = \begin{cases} 1 & l_{ij} \in \Psi_k \\ 0 & l_{ij} \notin \Psi_k \end{cases}. \quad (41)$$

By introducing the path-branch incidence matrix, the generalized modified DistFlow equations (33) and (34) become:

$$\hat{P}_{Br} = -T P_N W_R, \quad (42)$$

$$\hat{Q}_{Br} = -T Q_N W_R. \quad (43)$$

Then, according to (33)-(37) and path-branch incidence matrix, the matrix form of voltage equations can be obtained:

$$W_R = (2 - V_0) - (T^T R_N T P_N + T^T X_N T Q_N) W_R. \quad (44)$$

According to the definition of W , $V_R = 2 - W_R$, the voltage for

each bus can be obtained by:

$$V_R = 2 - (I + T^T R_N T P_N + T^T X_N T Q_N)^{-1} (2 - V_0). \quad (45)$$

Equation (45) is the closed-form relation between nodal voltage magnitudes and power injections for general distribution networks.

III. APPLICATIONS TO VAR OPTIMIZATION AND NETWORK RECONFIGURATION

A. Objective Functions

In this section, we apply the proposed modified DistFlow model to the VAR optimization and network reconfiguration problem. Our objective is to minimize the network loss, the operating cost, the voltage magnitude deviation, or their combinations. Thus, the objective function can be written as:

$$\min_{\substack{x_{ij}, \hat{Q}_i^C, V_i, W_i, \\ \hat{P}_i, \hat{Q}_i, \hat{P}_{ij}, \hat{Q}_{ij}}} \alpha \sum_{ij \in \Phi_L} R_{ij} (\hat{P}_{ij}^2 + \hat{Q}_{ij}^2) + \beta \sum_{ij \in \Phi_L} (x_{ij} - x_{ij}^0)^2 + \gamma \sum_{i \in \Phi_B} (V_i - 1)^2, \quad (46)$$

where the first term represents the network loss components. Note that the network loss of branch ij is calculated by:

$$\text{loss}_{ij} = R_{ij} \frac{P_{ij}^2 + Q_{ij}^2}{V_i^2} = R_{ij} (\hat{P}_{ij}^2 + \hat{Q}_{ij}^2). \quad (47)$$

The second term denotes the cost of switch operations, and β should be set as the switching cost. The third term represents the voltage deviations.

Decision variables herein are the status of branches x_{ij} , the reactive power output of shunt capacitors \hat{Q}_i^C , voltage magnitudes V_i and its auxiliary variables W_i , modified power injections \hat{P}_i and \hat{Q}_i , and modified branch flows \hat{P}_{ij} and \hat{Q}_{ij} . The first two terms are control variables, and other variables change accordingly.

B. Constraints

Besides, the following constraints need to be incorporated into the VAR optimization and network reconfiguration model.

1) Integer Variable and Constraints

Let binary variable x_{ij} denote the branch switch status (where $x_{ij} = 1$ indicates that switch ij is closed, whereas $x_{ij} = 0$ suggests that the switch ij is open).

$$x_{ij} \in \{0, 1\}, \quad \forall ij \in \Phi_L. \quad (48)$$

When a branch ij is open, i.e., $x_{ij} = 0$, its active and reactive power flow must be zero. Such limitations can be written in the following form of linear inequality constraints:

$$-x_{ij} \cdot M \leq \hat{P}_{ij} \leq x_{ij} \cdot M, \quad (49)$$

$$-x_{ij} \cdot M \leq \hat{Q}_{ij} \leq x_{ij} \cdot M. \quad (50)$$

2) Branch Flow Constraints

According to modified DistFlow, the branch flow constraints can be written as:

$$\sum_{i \in N_i} \hat{P}_{ij} + \hat{P}_j = 0, \quad \forall j \in \Phi_B, \quad (51)$$

$$\sum_{i \in N_i} \hat{Q}_{ij} + \hat{Q}_j = 0, \quad \forall j \in \Phi_B. \quad (52)$$

3) Voltage Constraints

According to modified DistFlow, for a closed branch, the voltage drop along the distribution line is:

$$W_j - W_i = R_{ij} \hat{P}_{ij} + X_{ij} \hat{Q}_{ij}, \quad \forall ij \in \Phi_L, \quad (53)$$

$$V_i = 2 - W_i, \quad \forall ij \in \Phi_L. \quad (54)$$

To incorporate the case with open branches, the big-M method is introduced [21] and the voltage constraints (53) become:

$$W_j - W_i \leq (1 - x_{ij})M + R_{ij} \hat{P}_{ij} + X_{ij} \hat{Q}_{ij}, \quad \forall ij \in \Phi_L, \quad (55)$$

$$W_j - W_i \geq -(1 - x_{ij})M + R_{ij} \hat{P}_{ij} + X_{ij} \hat{Q}_{ij}, \quad \forall ij \in \Phi_L. \quad (56)$$

4) Active and Reactive Power Injection Constraints

$$\hat{P}_i = -P_i^D W_i + \tilde{P}_i^G W, \quad \forall i \in \Phi_B, \quad (57)$$

$$\hat{Q}_i = -Q_i^D W_i + \tilde{Q}_i^G W + \hat{Q}_i^C, \quad \forall i \in \Phi_B. \quad (58)$$

5) VAR Compensators Operation Constraints

The constraints for static VAR compensators (SVC) are:

$$\underline{Q}_i^C W_i \leq \hat{Q}_i^C \leq \bar{Q}_i^C W_i, \quad \forall i \in \Phi_C. \quad (59)$$

6) Radiation Constraints

According to [22], the constraints for a radial topology can be obtained by:

$$\sum_{i \neq j} x_{ij} = N_{\text{node}} - N_{\text{root}}, \quad \forall ij \in \Phi_L. \quad (60)$$

7) Branch Power Flow Limits

Limits on active and reactive power flow:

$$-\bar{P}_{ij} W_i \leq \hat{P}_{ij} \leq \bar{P}_{ij} W_i, \quad \forall ij \in \Phi_L, \quad (61)$$

$$-\bar{Q}_{ij} W_i \leq \hat{Q}_{ij} \leq \bar{Q}_{ij} W_i, \quad \forall ij \in \Phi_L, \quad (62)$$

$$\hat{P}_{ij}^2 + \hat{Q}_{ij}^2 \leq \bar{I}_{ij}^2, \quad \forall ij \in \Phi_L. \quad (63)$$

According to the definition of \hat{P}_{ij} and \hat{Q}_{ij} , i.e., (38), the thermal limits of the branch can be presented by (63).

8) Bus Voltage Limits

$$2 - \bar{V}_i \leq W_i \leq 2 - \underline{V}_i, \quad \forall i \in \Phi_B. \quad (64)$$

9) Phase Angle Difference Limits

Since the modified DistFlow is based on Assumption 1, we make the following phase angle constraints according to (20):

$$-(2 - W_j) \sin \bar{\delta}_{ij} \leq X_{ij} \hat{P}_{ij} - R_{ij} \hat{Q}_{ij} \leq (2 - W_j) \sin \bar{\delta}_{ij}, \quad \forall ij \in \Phi_L. \quad (65)$$

We usually set $\bar{\delta}_{ij}$ to 10 degrees.

Note that the objective function (46) is a convex quadratic function. Equality constraints {(51), (52), (54), (57), (58), (60)} are affine and inequality constraints {(49), (50), (55), (56), (59), (61)-(64)} are convex. Thus the VAR optimization and network reconfiguration problem becomes a MIQP with the proposed modified DistFlow model.

C. Method to improve computational efficiency

The mixed-integer programming is usually solved by branch and cut algorithms, which suffers from a high computation burden in dealing with integer variables. The computation time for network reconfiguration will be reduced if the status of some branches can be predetermined.

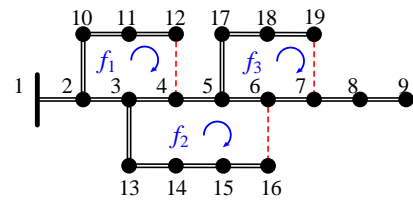


Fig. 5. A simple distribution system.

A simple distribution network is shown in Fig. 5 to introduce the basic concepts of the method. The normally closed branches are shown as double solid lines, and the normally opened

branches are displayed as red dashed lines.

Define two loops f_1 and f_2 are *overlapping* if $B_{f_1} \cap B_{f_2} \neq \emptyset$. If the two loops f_1 and f_2 are not overlapped with other loops, $\{f_1, f_2\}$ are overlapping loop set. For k th overlapping loop set, there are L_k branches in Θ_k should be opened otherwise there will be a loop in the network, meanwhile, the isolated island will happen at other places.

$$N_k - \sum x_{ij} = L_k, \forall ij \in \Theta_k. \quad (66)$$

Constraints (66) are necessary conditions for radial configuration, which could save time to judge whether a solution is feasible. This method is strict in mathematics and will not affect the optimality of the result.

IV. NUMERICAL TESTS

We tested the proposed modified DistFlow model and the VAR optimization and network reconfiguration technique, respectively. In all tests, the voltage magnitude of the power supply point (PSP) was set as 1.05 p.u. All simulations were tested in MATLAB on a laptop with an Intel Core i7-5600U 2.60GHz CPU and 8GB of RAM.

A. On the Linear Branch Flow Model

The proposed modified DistFlow model was compared with multiple benchmarks, including LPF-D [3], simplified DistFlow [15], as well as the ACPF model calculated by MATPOWER 7.1 [23]. We first chose the 33-bus system as our testbed. The results of voltage magnitudes, branch active power flows, and branch reactive power flows calculated by ACPF as well as the errors of modified DistFlow (MD), LPF-D, and SD were illustrated in Fig. 6-8, respectively.

Fig. 6 shows that the voltage magnitude results of MD are closest to ACPF. The average error and the largest error of MD were 0.008% and 0.014%, respectively. The average error and the largest error of LPF-D were 0.085% and 0.164%, respectively. The average error and the largest error of SD were 0.170% and 0.247% respectively. We also observed that errors grew larger when the voltage magnitude became lower. However, even the largest errors of MD were within a negligible range and were much smaller than LPF-D and SD.

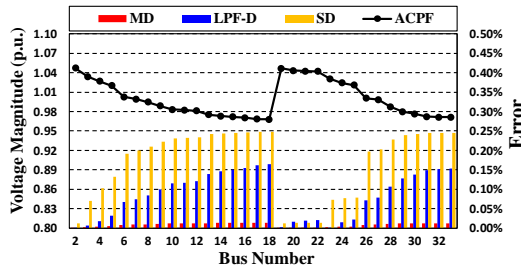


Fig. 6. Results of bus voltage magnitudes.

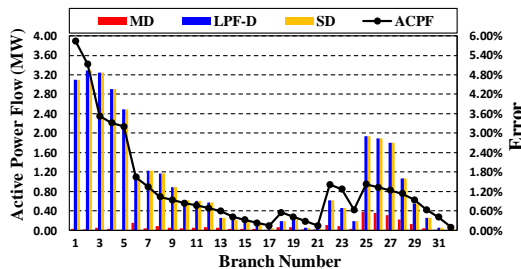


Fig. 7. Results of branch active power flows.

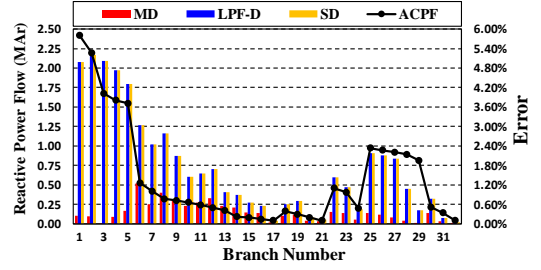


Fig. 8. Results of branch reactive power flows.

As shown in Figs. 7 and 8, the results of active and reactive branch flow from MD were also closest to ACPF. Its largest errors were 0.559% at branch 25 and 1.236% at branch 6 for active and reactive power flow, respectively. Its average errors were 0.118% and 0.351%. Compared to LPF-D and SD, the branch flow results of MD were much more accurate. Meanwhile, from Fig. 7-8, we observed that errors on active and reactive power flows for LPF-D and SD were the same, this is because they share the same branch flow equations by ignoring the quadratic term of network losses. (Please refer to (16)~(27) in [3] and (5.i, 5.ii) in [15]).

Subsequently, the proposed modified DistFlow model was tested and compared on a larger 141-bus system. Its mean and largest errors for voltage magnitudes, branch active power flows, and branch reactive power flows were recorded in TABLE I, along with the results of LPF-D and SD. From TABLE I, we can see that errors of MD were much smaller than those of LPF-D and SD.

TABLE I
POWER FLOW RESULTS COMPARISON ON IEEE 141-BUS SYSTEM

Error	Method	Bus Voltages	Branch Flows	
		V_i	P_{ij}	Q_{ij}
Average Error	MD	0.002%	0.024%	0.044%
	LPF-D	0.024%	0.334%	0.394%
	SD	0.129%	0.334%	0.394%
Largest Error	MD	0.003%	0.471%	0.407%
	LPF-D	0.064%	4.522%	5.350%
	SD	0.178%	4.522%	5.350%

The increasing electric vehicle charging demand potentially leads to overload [24]. To check the performance of the proposed modified DistFlow model heavier load conditions, we employed the 33-bus system and 141-bus system, and gradually increased the load power therein. Individually, loads of 33-bus systems were scaled up to 210%~250% of the baseload, and loads of 141-bus systems were scaled up to 260%~300% of the baseload. These values would gradually make the lowest voltage magnitude in the system close to 0.8 p.u. The mean and largest errors in voltage magnitudes, branch active power flows, and branch reactive power flows for all linear power flow models were compared in TABLE II.

In Table II, the lowest voltage decreased from 0.86 p.u. to as low as 0.81 p.u. From the table, it can be observed that the voltage error of MD was less affected by low voltage. When the voltage magnitude was around 0.8 p.u., the average and the largest errors of voltage magnitude were about 0.5% and 1%, respectively, and the errors of branch power flows were still acceptable. Whereas for LPF-D and SD, the errors of voltage

TABLE II
COMPARISONS AMONG MODIFIED DISTFLOW, LPF-D AND SIMPLIFIED DISTFLOW UNDER HEAVY LOAD SYSTEM

System	Load Level	Lowest V (p.u.)	Modified DistFlow						LPF-D						Simplified DistFlow					
			Error V (%)		Error P_{ij} (%)		Error Q_{ij} (%)		Error V (%)		Error P_{ij} (%)		Error Q_{ij} (%)		Error V (%)		Error P_{ij} (%)		Error Q_{ij} (%)	
			ϵ_V^{avg}	ϵ_V^{max}	$\epsilon_{P_{ij}}^{avg}$	$\epsilon_{P_{ij}}^{max}$	$\epsilon_{Q_{ij}}^{avg}$	$\epsilon_{Q_{ij}}^{max}$	ϵ_V^{avg}	ϵ_V^{max}	$\epsilon_{P_{ij}}^{avg}$	$\epsilon_{P_{ij}}^{max}$	$\epsilon_{Q_{ij}}^{avg}$	$\epsilon_{Q_{ij}}^{max}$	ϵ_V^{avg}	ϵ_V^{max}	$\epsilon_{P_{ij}}^{avg}$	$\epsilon_{P_{ij}}^{max}$	$\epsilon_{Q_{ij}}^{avg}$	$\epsilon_{Q_{ij}}^{max}$
33-Bus System	210%	0.860	0.213	0.397	0.615	2.359	1.170	3.766	1.324	2.455	3.581	11.601	4.253	12.187	1.088	1.681	3.581	11.601	4.253	12.187
	220%	0.849	0.266	0.496	0.709	2.623	1.305	4.093	1.541	2.861	3.814	12.325	4.529	12.921	1.244	1.934	3.814	12.325	4.529	12.921
	230%	0.837	0.330	0.617	0.814	2.909	1.453	4.443	1.783	3.316	4.057	13.073	4.816	13.677	1.419	2.220	4.057	13.073	4.816	13.677
	240%	0.825	0.406	0.762	0.930	3.221	1.614	4.817	2.054	3.827	4.311	13.848	5.116	14.458	1.615	2.544	4.311	13.848	5.116	14.458
	250%	0.813	0.497	0.938	1.060	3.562	1.790	5.218	2.357	4.401	4.576	14.654	5.429	15.266	1.835	2.912	4.576	14.654	5.429	15.266
141-Bus System	260%	0.850	0.237	0.466	0.133	1.657	0.315	3.173	1.611	2.934	1.046	13.359	1.217	15.500	1.350	2.042	1.046	13.359	1.217	15.500
	270%	0.840	0.287	0.565	0.154	1.917	0.346	3.509	1.823	3.325	1.102	14.013	1.281	16.236	1.506	2.295	1.102	14.013	1.281	16.236
	280%	0.830	0.346	0.682	0.176	2.203	0.379	3.873	2.056	3.756	1.160	14.684	1.347	16.989	1.678	2.577	1.160	14.684	1.347	16.989
	290%	0.820	0.415	0.820	0.202	2.517	0.414	4.268	2.310	4.232	1.220	15.374	1.416	17.761	1.866	2.890	1.220	15.374	1.416	17.761
	300%	0.809	0.495	0.982	0.229	2.862	0.452	4.695	2.590	4.758	1.282	16.084	1.486	18.552	2.074	3.239	1.282	16.084	1.486	18.552

magnitudes and branch power flows were several times as much as modified DistFlow, which verified the better performance of modified DistFlow under low voltage conditions.

B. VAR Optimization and Network Reconfiguration

Various cases considering DGs and SVCs were used to compare the performance of the MIQP model and MISOCP model [1] for VAR optimization and network reconfiguration problems, and the algorithms were solved by an embedded IBM CPLEX 12.8 solver with the YALMIP interface in MATLAB.

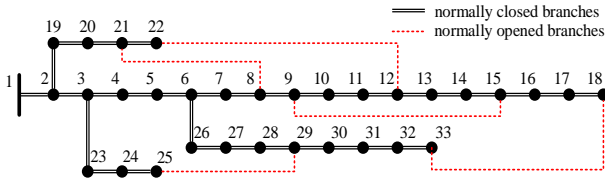


Fig. 9. The 33-bus system.

We first chose the 33-bus system as the testbed. In the VAR optimization and network reconfiguration, three objectives and three cases were tested to compare the MIQP model and the MISOCP model [1].

Objective I: Minimizing the active power losses.

Objective II: Minimizing the cost of network reconfiguration. The energy cost α was set as 30\$/MWh, and the switching cost β was estimated as 0.2\$.

Objective III: Minimizing the voltage deviation. The coefficient α and β were set as 0, and the γ was set as 100. To highlight the effect of network reconfiguration, loads of the whole system were scaled up to 150% of the baseload.

To diverse the testbed, we set three cases:

Case I: There was no DG and SVC in the system.

Case II: There was only one DG installed at Bus 10 with an output of 0.8 MW and 0.5 MVar.

Case III: There were two DGs at Bus 16 and 30 with an output of 0.5 MW and 0.25 MVar, and an SVC at Bus 22 within an output range of [-0.5, 0.5] MVar.

Combined with the objective functions and cases, there were totally nine scenarios. In these scenarios, we compared the MIQP proposed in this paper with the MISOCP proposed in [1] from the aspects of optimal value, optimal solution, and solution time. The comparison results were shown in Table III.

In scenarios 1-6, according to [13], minimizing the network losses as the objective function satisfies the relaxation condition of SOCP. Therefore, the solutions obtained by MISOCP, which are usually optimal, can be regarded as benchmarks. From Table III, we can see that the optimal value of MIQP is the same as MISOCP, and the branch status in the optimal solution of MIQP is consistent with that of MISOCP, which verifies the optimality and accuracy of MIQP. Meanwhile, it can be observed that the time costs of MIQP were much lower than MISOCP in all scenarios.

In scenarios 7-9, because the objective function of minimizing the voltage deviation does not satisfy the relaxation condition of SOCP, MISOCP is not applicable to this problem. While MIQP still solved these problems successfully.

From these results, we conclude that i) when the MISOCP model is applicable, the proposed MIQP model obtained the same results with much lower time costs, and ii) when the MISOCP model is not applicable, the proposed MIQP approach still solved the VAR optimization and network reconfiguration problem successfully.

To test the performance of the proposed MIQP model on large systems, a 981-bus system was adopted for testing, which combined seven 141-bus systems with different load levels and inter-area switch connections. To apply the MIQP algorithm on the system, we set up six normally open lines, which were represented by the red dashed line in the figure. Therefore, there

TABLE III
RESULTS OF IEEE 33-BUS SYSTEM

NO.	Objective function	Load Level	Case	MIQP					MISOCP				
				Obj. ¹	Loss(kW)	V_{avg} (p.u.)	Opened Branches	Time(s)	Obj.	Loss(kW)	V_{avg} (p.u.)	Opened Branches	Time(s)
1	Obj. 1	100%	I	125.36	125.36	1.017	7-8, 9-10, 14-15, 32-33, 25-29	3.56	125.36	125.36	1.017	7-8, 9-10, 14-15, 32-33, 25-29	9.89
2			II	81.92	81.92	1.024	6-7, 8-9, 14-15, 12-22, 25-29	5.01	81.92	81.92	1.024	6-7, 8-9, 14-15, 12-22, 25-29	6.71
3			III	53.58	53.58	1.032	7-8, 10-11, 14-15, 9-15, 25-29	3.49	53.58	53.58	1.032	7-8, 10-11, 14-15, 9-15, 25-29	7.52
4	Obj. 2 $C^p = 30$ $C^b = 0.2$	100%	I	4.53	137.66	1.014	8-9, 21-8, 9-15, 18-33, 25-29	1.72	4.53	137.66	1.014	8-9, 21-8, 9-15, 18-33, 25-29	1.72
5			II	3.04	101.31	1.019	21-8, 9-15, 12-22, 18-33, 25-29	0.86	3.04	101.31	1.019	21-8, 9-15, 12-22, 18-33, 25-29	1.21
6			III	2.15	71.83	1.024	21-8, 9-15, 12-22, 18-33, 25-29	0.37	2.15	71.83	1.024	21-8, 9-15, 12-22, 18-33, 25-29	0.64
7	Obj. 3 $\alpha = 0$ $\beta = 100$	150%	I	1.86	294.58	1.000	7-8, 9-10, 14-15, 32-33, 25-29	18.27	NOT APPLICABLE (infeasible power flow solution)				-
8			II	1.46	260.44	1.003	4-5, 10-11, 14-15, 28-29, 32-33	15.17	NOT APPLICABLE (infeasible power flow solution)				-
9			III	1.22	210.53	1.000	4-5, 8-9, 14-15, 27-28, 32-33	10.81	NOT APPLICABLE (infeasible power flow solution)				-

¹ the values of objective function and loss were calculated by ACPF results based on the branches' status that had been obtained by the MIQP problem.

were 986 lines in the system. To ensure the feasible solution of power flow calculation, we reduced the load in each system according to the ratio shown in Fig. 10.

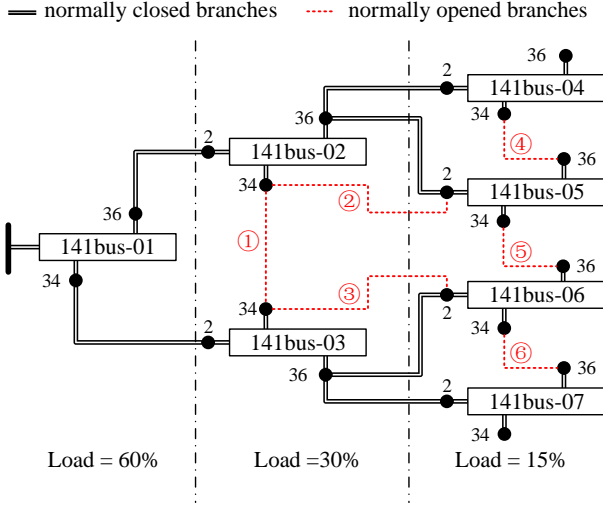


Fig. 10. A 981-bus system.

The proposed MIQP model and accelerate method were used to calculate the optimal topology and network losses. Subsequently, we used ACPF to calculate the power flow under the optimal topology to verify the accuracy of the MIQP model optimal solution. The result shows that it took 233.4 seconds to obtain the optimal solution, which confirmed that the proposed model and algorithm could be applied to VAR optimization network reconfiguration in large systems. In contrast, the MISOCP model failed to solve the VAR optimization and network reconfiguration issues for this system.

In summary, we conclude that the proposed modified DistFlow model is much more accurate than existing benchmarks, and the MIQP model based on modified DistFlow enjoys satisfactory accuracy and efficiency even for large systems.

V. CONCLUSION

In this paper, a cold-start LBF model named modified DistFlow is proposed by replacing the active and reactive power with their ratios to voltage magnitude as the state variables. Such a LBF model is applied to the problem of VAR optimization and network reconfiguration, transforming it to a MIQP. Theoretical analysis and numerical tests both show that the proposed modified DistFlow has an outstanding accuracy, and the resulting MIQP model for VAR optimization and network reconfiguration is very efficient to solve and can be applied to a wide range of problems. We also look forward to solving more distribution system problems with the modified DistFlow model as our basic tool in the future.

REFERENCES

- [1] Z. Tian, W. Wu, B. Zhang, and A. Bose, "Mixed-integer second-order cone programming model for VAR optimisation and network reconfiguration in active distribution networks," *IET Generation, Transmission & Distribution*, vol. 10, no. 8, pp. 1938-1946, 2016.
- [2] T. Ding, S. Liu, W. Yuan, Z. Bie, and B. Zeng, "A two-stage robust reactive power optimization considering uncertain wind power integration in active distribution networks," *IEEE Transactions on Sustainable Energy*, vol. 7, no. 1, pp. 301-311, 2015.
- [3] H. Yuan, F. Li, Y. Wei, and J. Zhu, "Novel linearized power flow and linearized OPF models for active distribution networks with application in distribution LMP," *IEEE Transactions on Smart Grid*, vol. 9, no. 1, pp. 438-448, 2016.
- [4] K. Purchala, L. Meeus, D. Van Dommelen, and R. Belmans, "Usefulness of DC power flow for active power flow analysis," *IEEE Power Engineering Society General Meeting*, pp. 454-459, 2005.
- [5] H. Sun, Q. Guo, B. Zhang, W. Wu, and B. Wang, "An adaptive zone-division-based automatic voltage control system with applications in China," *IEEE Transactions on Power Systems*, vol. 28, no. 2, pp. 1816-1828, 2012.
- [6] X. Chen, W. Wu, and B. Zhang, "Robust capacity assessment of distributed generation in unbalanced distribution networks incorporating ANM techniques," *IEEE Transactions on Sustainable Energy*, vol. 9, no. 2, pp. 651-663, 2017.
- [7] J. Zhang, M. Cui, B. Li, H. Fang, and Y. He, "Fast Solving Method Based on Linearized Equations of Branch Power Flow for Coordinated Charging of EVs (EVCC)," *IEEE Transactions on Vehicular Technology*, vol. 68, no. 5, pp. 4404-4418, 2019.
- [8] S. Gharebaghi, A. Safdarian, and M. Lehtonen, "A Linear Model for AC Power Flow Analysis in Distribution Networks," *IEEE Systems Journal*, vol. 13, no. 4, pp. 4303-4312, 2019.
- [9] Z. Li, J. Yu, and Q. Wu, "Approximate linear power flow using logarithmic transform of voltage magnitudes with reactive power and transmission loss consideration," *IEEE Transactions on Power Systems*, vol. 33, no. 4, pp. 4593-4603, 2017.
- [10] J. Yang, N. Zhang, C. Kang, and Q. Xia, "A State-Independent Linear Power Flow Model With Accurate Estimation of Voltage Magnitude," *IEEE Transactions on Power Systems*, vol. 32, no. 5, pp. 3607-3617, 2017.
- [11] A. Garces, "A linear three-phase load flow for power distribution systems," *IEEE Transactions on Power Systems*, vol. 31, no. 1, pp. 827-828, 2015.
- [12] S. Bolognani, and S. Zampieri, "On the Existence and Linear Approximation of the Power Flow Solution in Power Distribution Networks," *IEEE Transactions on Power Systems*, vol. 31, no. 1, pp. 163-172, 2016.
- [13] M. Farivar, and S. H. Low, "Branch Flow Model: Relaxations and Convexification—Part I," *IEEE Transactions on Power Systems*, vol. 28, no. 3, pp. 2554-2564, 2013.
- [14] M. Farivar, and S. H. Low, "Branch Flow Model: Relaxations and Convexification—Part II," *IEEE Transactions on Power Systems*, vol. 28, no. 3, pp. 2565-2572, 2013.
- [15] M. E. Baran, and F. F. Wu, "Network reconfiguration in distribution systems for loss reduction and load balancing," *IEEE Power Engineering Review*, vol. 9, no. 4, pp. 101-102, 1989.
- [16] Q. Peng, Y. Tang, and S. H. Low, "Feeder reconfiguration in distribution networks based on convex relaxation of OPF," *IEEE Transactions on Power Systems*, vol. 30, no. 4, pp. 1793-1804, 2014.
- [17] M. R. Dorostkar-Ghamsari, M. Fotuhi-Firuzabad, M. Lehtonen, and A. Safdarian, "Value of distribution network reconfiguration in presence of renewable energy resources," *IEEE Transactions on Power Systems*, vol. 31, no. 3, pp. 1879-1888, 2015.
- [18] Z. Yang, K. Xie, J. Yu, H. Zhong, N. Zhang, and Q. Xia, "A general formulation of linear power flow models: Basic theory and error analysis," *IEEE Transactions on Power Systems*, vol. 34, no. 2, pp. 1315-1324, 2018.
- [19] B. Zhang, and Z. Yan, *Advanced electric power network analysis*: Cengage Learning Asia, 2011.
- [20] S. Xin, Q. Guo, H. Sun, C. Chen, J. Wang, and B. Zhang, "Information-energy flow computation and cyber-physical sensitivity analysis for power systems," *IEEE Journal on Emerging Selected Topics in Circuits Systems*, vol. 7, no. 2, pp. 329-341, 2017.
- [21] J. A. Taylor, and F. S. Hover, "Convex Models of Distribution System Reconfiguration," *IEEE Transactions on Power Systems*, vol. 27, no. 3, pp. 1407-1413, 2012.
- [22] M. Lavorato, J. F. Franco, M. J. Rider, and R. Romero, "Imposing Radiality Constraints in Distribution System Optimization Problems," *IEEE Transactions on Power Systems*, vol. 27, no. 1, pp. 172-180, 2012.
- [23] R. D. Zimmerman, C. E. Murillo-Sánchez, and R. J. Thomas, "MATPOWER: Steady-state operations, planning, and analysis tools for power systems research and education," *IEEE Transactions on power systems*, vol. 26, no. 1, pp. 12-19, 2010.
- [24] A. Palomino, M. Parvania, and Energy, "Data-Driven Risk Analysis of Joint Electric Vehicle and Solar Operation in Distribution Networks," *IEEE Open Access Journal of Power*, vol. 7, pp. 141-150, 2020.